Title

Polypeptide-Based Gold Nanoshells for Photothermal Therapy

Journal

SLAS TECHNOLOGY, 22(1)

ISSN

2472-6303

Authors

Mayle, Kristine M

Dern, Kathryn R

Wong, Vincent K

et al.

Publication Date

2017-02-01

DOI

10.1177/2211068216645292

Peer reviewed

Journal of Laboratory Automation
1–8

DOI: 10.1177/2211068216645292
jala.sagepub.com
SAGE

Polypeptide-Based Gold Nanoshells for Photothermal Therapy

Kristine M. Mayle[1], Kathryn R. Dern[1], Vincent K. Wong[1], Shijun Sung[2], Ke Ding[1], April R. Rodriguez[1], Zachary Taylor[1,3], Z. Hong Zhou[1,4,5], Warren S. Grundfest[1,2,3], Timothy J. Deming[1], and Daniel T. Kamei[1]

Abstract

Targeted killing of cancer cells by engineered nanoparticles holds great promise for noninvasive photothermal therapy applications. We present the design and generation of a novel class of gold nanoshells with cores composed of self-assembled block copolypeptide vesicles with photothermal properties. Specifically, poly(L-lysine)$_{60}$-*block*-poly(L-leucine)$_{20}$ ($K_{60}L_{20}$) block copolypeptide vesicles coated with a thin layer of gold demonstrate enhanced absorption of light due to surface plasmon resonance (SPR) in the near-infrared range. We show that the polypeptide-based $K_{60}L_{20}$ gold nanoshells have low toxicity in the absence of laser exposure, significant heat generation upon exposure to near-infrared light, and, as a result, localized cytotoxicity within the region of laser irradiation in vitro. To gain a better understanding of our gold nanoshells in the context of photothermal therapy, we developed a comprehensive mathematical model for heat transfer and experimentally validated this model by predicting the temperature as a function of time and position in our experimental setup. This model can be used to predict which parameters of our gold nanoshells can be manipulated to improve heat generation for tumor destruction. To our knowledge, our results represent the first ever use of block copolypeptide vesicles as the core material of gold nanoshells.

Keywords

polypeptide vesicles, photothermal therapies, gold nanoshells, cancer, nanoparticles

Introduction

Photothermal therapy holds great promise for treating cancer. In this approach, cancer cells are killed by heat generation caused by the conversion of light energy to heat by nanosized metallic particles. When a metal nanoparticle is exposed to light, the oscillating electromagnetic field of light induces a collective oscillation of the free electrons (conduction band electrons) of the metal.[1] The frequency of light at which the oscillation is a maximum is known as the surface plasmon resonance (SPR). The SPR of gold nanoparticles is dependent on the nanoparticle size and shape, as well as the dielectric properties of the surrounding medium. Optical properties can therefore be tuned by adjusting these parameters.[1]

SPR enhances all radiative and nonradiative properties of the gold nanoparticles, making them excellent scatterers and absorbers of light.[1–4] Absorption of light occurs when the photon energy causes electron oscillations in the matter, while scattering of light occurs when the photon energy is dissipated due to inelastic properties, which emit photons in the form of scattered light either at the same frequency as the incident light or at a shifted frequency. The ratio of scattering to absorption is important when choosing an application for the nanoparticles. For example, high scattering of light enables cellular imaging, while a high absorption of light is required to generate thermal energy for photothermal therapy.[2]

For photothermal therapy, it is desirable to develop gold nanoparticles that are responsive to near-infrared light to minimize attenuation of the energy due to light-tissue interactions.[5]

[1]Department of Bioengineering, University of California, Los Angeles, CA, USA
[2]Department of Electrical Engineering, University of California, Los Angeles, CA, USA
[3]Department of Surgery, University of California, Los Angeles, CA, USA
[4]Department of Microbiology, Immunology & Molecular Genetics, University of California, Los Angeles, CA, USA
[5]California NanoSystems Institute, University of California, Los Angeles, CA, USA

Received January 26, 2016.

Supplementary material for this article is available on the *Journal of Laboratory Automation* Web site at http://jla.sagepub.com/supplemental.

Corresponding Author:
Daniel T. Kamei, California NanoSystems Institute, University of California, 420 Westwood Plaza, Los Angeles, CA 90095, USA.
Email: kamei@seas.ucla.edu

In the near-infrared region, the absorption of light by tissue chromophores, such as hemoglobin and water, is minimal. Therefore, compared to visible and UV wavelengths of light, near-infrared light can penetrate deeper into tissue while maintaining the critical power density necessary for therapeutic effect, and damage to tissue is minimal. To obtain SPR in the near-infrared band, researchers have developed gold nanoparticles of different shapes and sizes, such as gold nanorods[2] and gold nanoshells.[6] Gold nanoshells, which are characterized by a thin layer of gold deposited onto a dielectric core, have demonstrated SPR bands ranging from UV to the mid-infrared region, with the wavelength depending on the core diameter and shell thickness.[6]

There are several methods to creating gold nanoshells, which typically use an aminated or thiolated core material on which to coat a thin layer of gold. The classic method for creating gold-coated silica nanoparticles is a several-step process.[6,7] In this method, small gold colloids (2–3 nm in diameter) are seeded onto aminated silica nanoparticles through the formation of dative bonds between the gold and surface amines. The gold shell is then completed through a gold plating process, in which gold ions in solution are reduced onto the seeded gold colloids.[6] More recently, gold nanoshells have been made through the direct reduction of gold ions onto a functionalized core material using a gentle reducing agent, such as hydroxylamine. The reduction of gold ions by hydroxylamine is accelerated by the presence of gold surfaces being formed on the functionalized core material, resulting in the absence of external nucleation/gold colloid formation, as all the Au^{3+} goes to the formation of the nanoshells.[8,9] External nucleation can cause high heterogeneity in the sample and lead to poor characterization of the desired nanoshell population. The desired SPR wavelength of the gold nanoshells can be tuned by adjusting the amount of gold ions added, the pH of the reduction reaction, the core diameter, and the composition of the dielectric core material.

The properties of the core material, such as the dielectric constant, can affect the optical properties of the gold nanoshells, including the absorption efficiency, plasmon line width, and plasmon energies.[10] The core material of the first gold nanoshell was a solid silica nanoparticle; however, other materials have also been used as core materials, such as polymeric and semiconductor nanoparticles.[6,11–13] Furthermore, liposomes have been explored as a core material, since they can provide additional benefits such as encapsulation of hydrophilic and hydrophobic cargo in the core and bilayer, respectively. Gold nanoshells with liposome cores have shown promise in photothermal therapy. In addition, other laboratories have shown that photothermal-capable gold-based nanostructures can be coupled with other applications such as triggered release of anticancer drugs and gene expression profiling in cells.[9,14–17]

Here we present the development of gold nanoshells using a novel core material: polypeptide vesicles. Polypeptide vesicles are an emerging class of biomaterials that have shown promise in delivering cargo, such as nucleic acids and anticancer drugs,[18–20] and this work represents its first use as a core material for gold nanoshells. Vesicles formed from amphiphilic block copolypeptides can provide increased stability over conventional liposomes, since the formation of thicker vesicle membranes contributes to increased attractive interactions between the building blocks. Furthermore, block copolypeptides with a wide variety of chemical and physical properties have been synthesized from naturally occurring and/or synthetic amino acid residues using transition metal–initiated ring opening polymerization of *N*-carboxyanhydrides. Since polypeptide vesicles are made from amino acid building blocks, they have the potential to exhibit low immunogenicity and toxicity. In this work, we investigated the use of the poly(L-lysine)$_{60}$-*block*-poly(L-leucine)$_{20}$ block copolypeptide ($K_{60}L_{20}$) vesicles as a novel class of core materials for hollow gold nanoshells.

Previously, the Deming research group examined the ability of the $K_{60}L_{20}$ block copolypeptides to self-assemble into vesicular structures, which could be extruded to a 100- to 200-nm size with low polydispersity.[18] While the $K_{60}L_{20}$ vesicles were able to encapsulate hydrophilic cargo,[18] the use of the positively charged vesicles as a drug delivery vehicle was limited due to its high cytotoxicity. We reasoned that coating the vesicles with gold would enable their use for photothermal therapy as the gold shell would mask the charges of the surface amines, which interact strongly with the net negatively charged cell membrane to induce cellular damage, and gold nanoparticles are known to be relatively nontoxic to cells. To efficiently coat the $K_{60}L_{20}$ vesicles with gold, we took advantage of the abundance of amines on the vesicle surface, provided by the 60 residues of lysine in the hydrophilic block of the copolypeptides. Optimization of the gold coating allowed for tunability of the SPR to the near-infrared region. Furthermore, as predicted, the gold-coated $K_{60}L_{20}$ vesicles demonstrated no discernible toxicity and significant heat generation upon exposure to quasi-coherent 808-nm irradiation. This resulted in substantial laser-induced cytotoxicity for in vitro photothermal therapy experiments.

Materials and Methods

Materials

PC3 cell lines were obtained from the American Type Culture Collection (Manassas, VA). Roswell Park Memorial Institute (RPMI) 1640 cell culture media, penicillin-streptomycin (P/S), sodium pyruvate (NaPyr), phosphate-buffered saline (PBS), and 0.25% trypsin with ethylenediaminetetraacetic acid (EDTA) were purchased from Invitrogen (Carlsbad, CA). Fetal bovine serum (FBS) was obtained from HyClone (Waltham, MA). The 96-well plates were purchased from Sigma-Aldrich (St. Louis, MO). The MTS cell proliferation

assay kit was purchased from Promega (Madison, WI). The Bradford reagent was obtained from Bio-Rad (Hercules, CA).

Synthesis of Block Copolypeptides

The $K_{60}L_{20}$ block copolypeptide was synthesized using the transition metal–initiated ring opening polymerization of *N*-carboxyanhydride as previously described.[18] The resulting copolypeptide was freeze-dried. The $K_{60}L_{20}$ polypeptide was processed into vesicles using a modification of a method previously reported.[18] Specifically, the vesicles were formed by first dissolving 10 mg polypeptide in 1 mL of a 15% tetrahydrofuran (THF) solution in sterile Milli-Q water (Millipore, Billerica, MA). Subsequently, another 1 mL of a 15% THF solution was added to yield a final polypeptide concentration of 0.5% w/v. The mixture was placed in a dialysis bag (molecular weight cut-off of 8000 Da) and dialyzed against sterile Milli-Q water overnight to remove the THF, where the sterile Milli-Q water was changed every hour for the first 4 h. The resulting vesicles were extruded through a series of polycarbonate membranes with 1000-, 400-, 200-, and 100-nm pores (in that order) to obtain more uniformly sized vesicles. The sizes of the vesicles and their distribution were analyzed with dynamic light scattering (DLS), and the Bradford assay was performed to quantify the final concentration of the polypeptide vesicles according to the manufacturer-supplied instructions, using the predialyzed samples as the standard.

Coating of Gold Nanoshells

A 2.7-mL suspension of polypeptide vesicles (0.782 mg) was adjusted to pH 7 using 7% ammonium hydroxide (Sigma-Aldrich). Hydroxylamine hydrochloride (Sigma-Aldrich) was added in excess (500 µL of a 0.2 M solution) followed by 90 µL of a 0.5% gold (III) chloride solution (Sigma-Aldrich) in two 45-µL aliquots. The suspension was allowed to spin for 2 h, and then 108 µL of a 0.5% gold (III) chloride solution was added in two 54-µL aliquots. The suspension was allowed to spin overnight, and the gold-coated vesicles were recovered by centrifugation at 9000 rcf for 10 min. The pH was determined to be critical in the gold-coating process, so the pH was adjusted as needed to maintain a pH of 7 throughout the coating process.

Characterization of Gold Nanoshells

Size and zeta potential measurements were performed on $K_{60}L_{20}$ vesicles with the Malvern Zetasizer Nano ZS model Zen 3600 (Malvern Instruments, Westborough, MA). For the transmission electron microscopy (TEM) and scanning electron microscopy (SEM) images, the colloidal gold nanoshells were first fully mixed by pipetting for a few times and immediately applied to carbon-coated copper grids. The grids were air-dried without staining or blotting. The TEM and SEM images were then recorded inside an FEI (Hillsboro, Oregon) T20 200kV transmission electron microscope and Zeiss (Oberkochen, Germany) Supra 40VP SEM, respectively. The extinction profile of the gold nanoshells was measured to verify the strong surface plasmon resonance in the near-infrared region using a UV-visible spectrophotometer (BioMate 3S; Thermo Scientific, Waltham, MA) over a range of wavelengths from 400 to 1100 nm.

Measuring Heat Generation

Gold nanoshells (extinction at 808 nm = 0.6 a.u.) were irradiated with an 808-nm laser diode (200 mW) (ThorLabs, Newton, NJ) for 10 min, at a power density of approximately 33 W cm^{-2}. The temperature was measured at desired time points using a thermocouple (model HYP-0; OMEGA Engineering, Stamford, CT) placed into a 96-well plate in 100 µL of the gold nanoshell solution suspended in water. The thermocouple could accurately measure temperature from cryogenic to 200 °C.

Mathematical Model for Heat Transfer of Gold Nanoshells

A model for the heating of the well due to laser irradiation of the gold nanoshells was developed by using the differential form of the conservation of energy equation. In this model, we assume that only the gold nanoshells within the path of the laser generate heat, and the heat is then conducted to the region outside of the path of the laser. For this approach, we defined two regions. The region in the path of the laser (the inner cylinder) was modeled using equation (1), while the region outside of this path (the cylindrical annulus) was modeled with equation (2).

$$\rho C_p \frac{\partial T}{\partial t} = k\nabla^2 T + Q_{laser}. \quad (1)$$

$$\rho C_p \frac{\partial T}{\partial t} = k\nabla^2 T. \quad (2)$$

The $\rho C_p \frac{\partial T}{\partial t}$ term on the left-hand side is related to the change in energy with respect to time of a differential volume of solution. The $k\nabla^2 T$ term on the right-hand side is associated with heat conduction, and equation (1) has an additional term, Q_{laser}, which is associated with the heat generated due to plasmonic heating of the gold nanoshells due to laser irradiation. In these equations, T is temperature (K), t is time (s), k is the thermal conductivity (W m^{-1} K^{-1}), ρ is the density (kg m^{-3}), C_p is the heat capacity (J kg^{-1} K^{-1}),

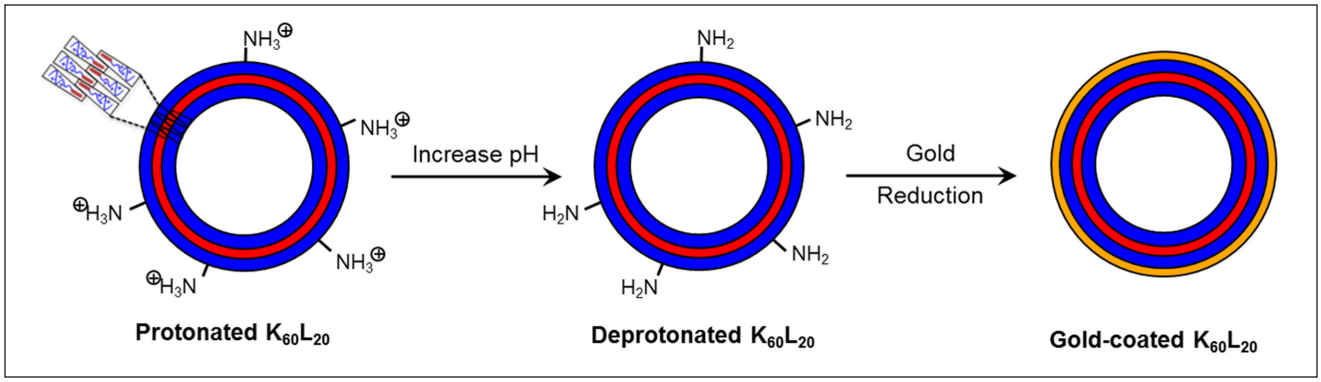

Figure 1. Schematic for making polypeptide-based gold nanoshells.

and Q_{laser} (W m^{-3}) is the heat generated by the gold nanoshells. The parameters used in the model are shown in **Supplemental Table S1**, and more details of the model can be found in the Supporting Information.

For this model, we solved the partial differential equation in both defined regions (inner cylinder and outer annulus) using finite difference equations and the method of lines coded in the MATLAB programming language.

Photothermal Therapy

PC3 cells were seeded onto 96-well plates at a density of 88,000 $cellcm^{-1}$. Gold nanoshells (extinction at 808 nm = 0.6 a.u.) were incubated with PC3 prostate cancer cells for 2 h in serum-free media. Cells were then irradiated with an 808-nm laser diode (200 mW) for 10 min. A Live/Dead Stain Kit (calcein AM and ethidium homodimer; Molecular Probes, Sunnyvale, CA) was then used to evaluate the viability of the cells. Cells were examined using fluorescent microscopy with the EVOS fl Digital Inverted Fluorescence Microscope (Advanced Microscopy Group/Life Technologies, Grand Island, NY).

Results and Discussion

Making Polypeptide-Based Gold Nanoshells

Typically, aminated core materials have been used for gold nanoshells, since amines can form dative bonds with gold to form a gold coating. On the basis of the success of such aminated core materials, we chose to develop the polypeptide-based gold nanoshell using the $K_{60}L_{20}$ vesicles, which have an abundance of lysines on the surfaces (**Fig. 1**). Using hydroxylamine to reduce the gold ions onto the surfaces of the vesicles, the $K_{60}L_{20}$ gold nanoshells were developed.

The SPR of gold nanoshells can be tuned to the near-infrared band by adjusting the ratio of the shell thickness to vesicle diameter. The diameter of the poly(L-lysine)$_{60}$-*block*-poly(L-leucine)$_{20}$ copolypeptide ($K_{60}L_{20}$) vesicles was established at approximately 122 nm by serial extrusion through polycarbonate membranes. As shown in **Figure 2**, the $K_{60}L_{20}$ gold nanoshells have an extinction peak close to the near-infrared region, where extinction is defined as the sum of the absorbance and scattering of light by the gold nanoshells. This indicated that light in the near-infrared range (e.g., 808-nm diode laser) could be used for triggering a therapeutic response. Although the peak does not correspond to 808 nm, the relatively high absorbance at 808 nm is still enough to induce cytotoxic effects. In the future, the absorbance peak can be shifted further into the near-infrared range by adjusting the core radius to shell thickness ratio of our gold nanoshells.[21] The extinction profile presented in **Figure 2** represents the effect of all nanoshells in the suspension.

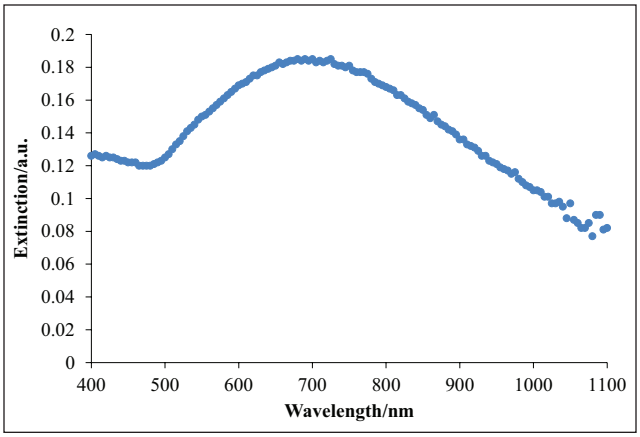

Figure 2. Visible near-infrared absorption spectra of the optimized polypeptide-based gold nanoshells. Extinction is the sum of the absorption and scattering of light in absorbance units (a.u.). Relative to gold nanorods, the broadening of the extinction profile can be attributed to the nonuniform size distribution of the $K_{60}L_{20}$ vesicles after the extrusion process.[29]

Based on DLS measurements, the gold nanoshells were found to be 150 nm in diameter and relatively monodisperse. Furthermore, the gold nanoshells were within the size range

Table 1. Characterization of Polypeptide-Based Gold Nanoshells.

$K_{60}L_{20}$ Vesicles	Size (nm)	Polydispersity Index
Uncoated	122 ± 1	0.252 ± 0.01
Coated	150 ± 2	0.125 ± 0.02

necessary to enable passive targeting of tumor tissue through the enhanced permeability and retention (EPR) effect (**Table 1**).[22] TEM and SEM images confirmed spherical gold nanoshells (**Fig. 3**), where the diameter of the gold nanoshells observed with TEM was also similar to those measured with DLS. Smaller sized gold nanoshells in the images can be attributed to smaller sized $K_{60}L_{20}$ vesicles and even $K_{60}L_{20}$ micelles. In our extrusion process, these smaller entities cannot be filtered out. A potential solution would be to use dialysis to remove some of the smaller self-assembled structures. The TEM and SEM images also show some possible aggregates, but these are most likely formed during the drying stages of the sample prior to imaging.[23] Images also indicate some nonuniformity in the thickness of the nanoshells. This might have been caused by the relatively high concentration of the hydroxylamine reducing agent, which may have led to greater local concentrations of the reducing agent that promoted rapid reduction of gold onto the vesicle surfaces in certain regions of the suspension. To correct this problem, the concentration of hydroxylamine can be reduced to decrease the probability that there will be regions of high hydroxylamine concentration, which could lead to more uniform gold coat thickness on all of the vesicles.

Furthermore, the zeta potential of the gold nanoshells, which is the electrostatic potential at the no-slip boundary of the nanoparticle, was measured to be +50 mV, indicating that the gold nanoshells exhibited a positive surface charge, enabling them to interact favorably with the net negatively charged cell membrane.

Due to the strong cellular membrane interaction, positively charged carriers can be highly cytotoxic. Previous attempts to use the positively charged, uncoated $K_{60}L_{20}$ vesicles for drug delivery had been limited due to a dose-dependent toxicity. Gold nanoparticles, on the other hand, are known to be relatively inert and nontoxic in vitro and in vivo. After coating the $K_{60}L_{20}$ vesicles with gold, they were found to be nontoxic to cells at all concentrations tested (Supporting Information). It is hypothesized that the addition of the gold coating disguised the lysine amino acids, resulting in a reduction of the overall toxicity.

Measuring Heat Generation from Gold Nanoshells

For photothermal therapy, near-infrared light that maximally overlaps with the SPR of the gold nanoshells can be used as an external trigger. The energy absorbed by the gold nanoshells is dissipated to the surrounding environment as heat. Research has shown that cancer cells are more sensitive to temperature increases, compared to normal cells, due to the harsh microenvironment corresponding to low partial pressures of oxygen and acidic pH conditions, where temperatures above 42 °C (315 °K) have been shown to effectively destroy tumor tissue in photothermal therapy.[24] The aqueous suspension containing $K_{60}L_{20}$ gold nanoshells showed a 28 K average temperature increase over a 10-min (600 s) exposure to the 808-nm (200 mW, approximately 33 W cm^{-2}) continuous-wave (CW) diode laser, and as expected, water alone showed a minimal average temperature increase from 20.5 to 21.9 °C upon laser irradiation (**Fig. 4**). Comparatively, the 28 K temperature increase with the gold nanoshells showed a significant increase in heat generation. These results demonstrate that our polypeptide-based gold nanoshells show promise as a triggered, local photothermal therapy.

Mathematical Modeling of the Heat Transfer Associated with $K_{60}L_{20}$ Gold Nanoshells

The heat generation by the gold nanoshells is a result of their strong absorbance of photons in the near-infrared

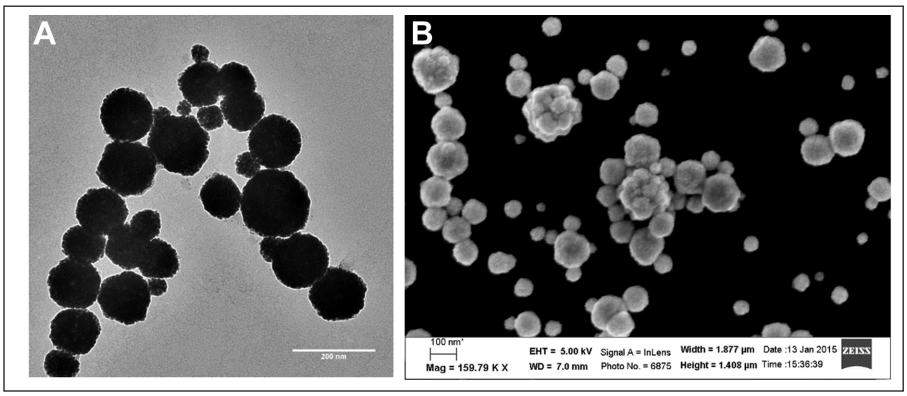

Figure 3. Images of the optimized $K_{60}L_{20}$ gold nanoshells. (**A**) Transmission electron microscopy image, scale bar = 200 nm. (**B**) Scanning electron microscopy image, scale bar = 100 nm.

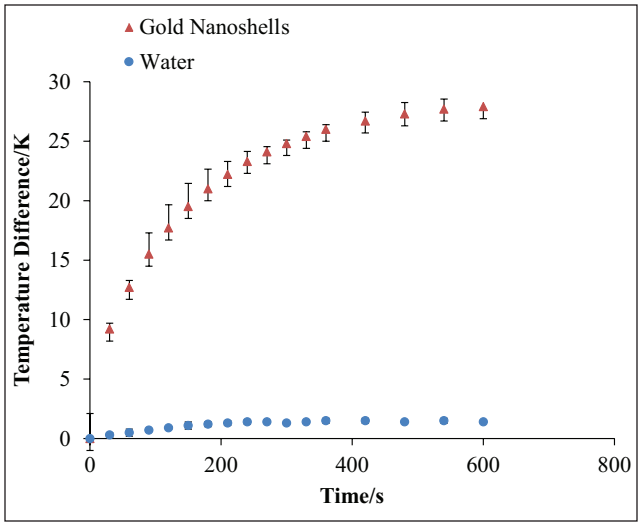

Figure 4. The temperature difference as a function of time for gold nanoshells in water with exposure to an 808-nm laser diode (200 mW). Data for gold nanoshells in water are represented by triangles, while data for water alone are represented by the circles. The error bars correspond to standard deviations from triplicate measurements. In the case of water, the error bars are smaller than the circle symbols.

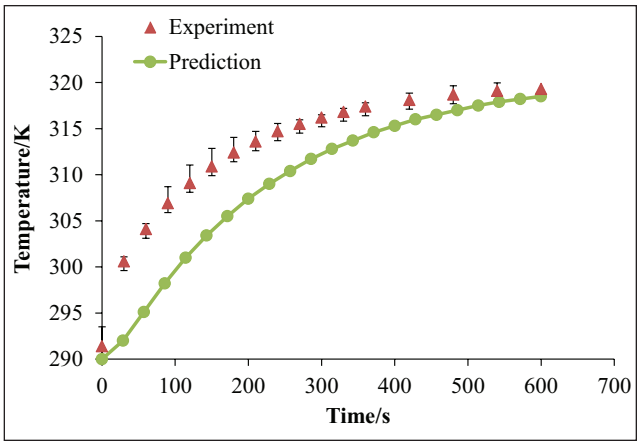

Figure 5. Comparison of our mathematical model predictions (circles) with our measured temperatures (triangles) for gold nanoshells in water with exposure to an 808-nm laser diode (200 mW). The error bars on the experimental data correspond to standard deviations from triplicate measurements.

region and subsequent conversion of the energy to heat. Several factors can affect the heat generation of gold nanoshells, including the diameter of the gold nanoshell (which can affect the optical properties, such as absorption cross section and efficiency), gold nanoshell concentration, and laser power density. Researchers have developed quantitative models to predict temperatures attained within well plates, cells in vitro, mock tumor phantoms, and tumors in vivo under a variety of parameters and conditions.[24–26]

To gain a better understanding of our $K_{60}L_{20}$ gold nanoshells in the context of photothermal therapy, we developed a comprehensive mathematical model for heat transfer. Such a model can be used in the future to determine which parameters can be manipulated to improve heat generation and, therefore, the destruction of tumors. The mathematical model was solved numerically using finite difference equations and the method of lines coded in the MATLAB programming language. This model was used to predict the increase in temperature observed in our in vitro laser irradiation experiments.

Using the mathematical model, the temperature increase as a function of time for the gold nanoshells was predicted, and the predictions were compared with the measured temperatures. As shown in **Figure 5**, the model reasonably predicted the increase in temperature. The slightly slower rise in our temperature predictions can be attributed to $\dot{m}$, the rate of evaporation. In reality, evaporation is less likely to occur at the beginning of heat generation, when temperatures are lower. However, in the model, an average rate of evaporation was assumed throughout the process. This overestimation in evaporation rate in the beginning is the most likely cause of our model's underprediction of heat generation as evaporation is associated with heat removal. We envision using the model in the future to determine how we can engineer our gold nanoshells to improve heating properties. For example, in the current mathematical model, Q_{laser} is related to the absorbance of our gold nanoshells and is an input that can be manipulated through engineering the design of the nanoshells. The ultimate goal of the model is to enable improvement of heat generation, which, in turn, would lead to greater photothermal treatment efficacy.

Photothermal Therapy Using Polypeptide-Based Gold Nanoshells

Hyperthermia treatment of cancer cells uses elevated temperatures above 42 °C, which can denature proteins and disrupt cell membranes.[27,28] Gold nanoshells can provide localized heating to the tumor site in response to near-infrared laser irradiation. To investigate the use of the $K_{60}L_{20}$ gold nanoshells for in vitro cytotoxicity, we incubated the gold nanoshells with prostate cancer cells for 2 h prior to laser irradiation. The results demonstrate that combination of $K_{60}L_{20}$ gold nanoshells and exposure to the near-infrared laser results in cytotoxicity, where the green and red stains indicate live and dead cells, respectively (**Fig. 6A,B**). Furthermore, the cell death is limited to the region of cells irradiated by the laser. In addition, no similar region is observed when cells are irradiated with the laser without the gold nanoshells (**Fig. 6C,D**). These promising in vitro results indicate that the $K_{60}L_{20}$ gold nanoshells can generate sufficient heat under near-infrared irradiation to cause localized cytotoxicity of cancer cells.

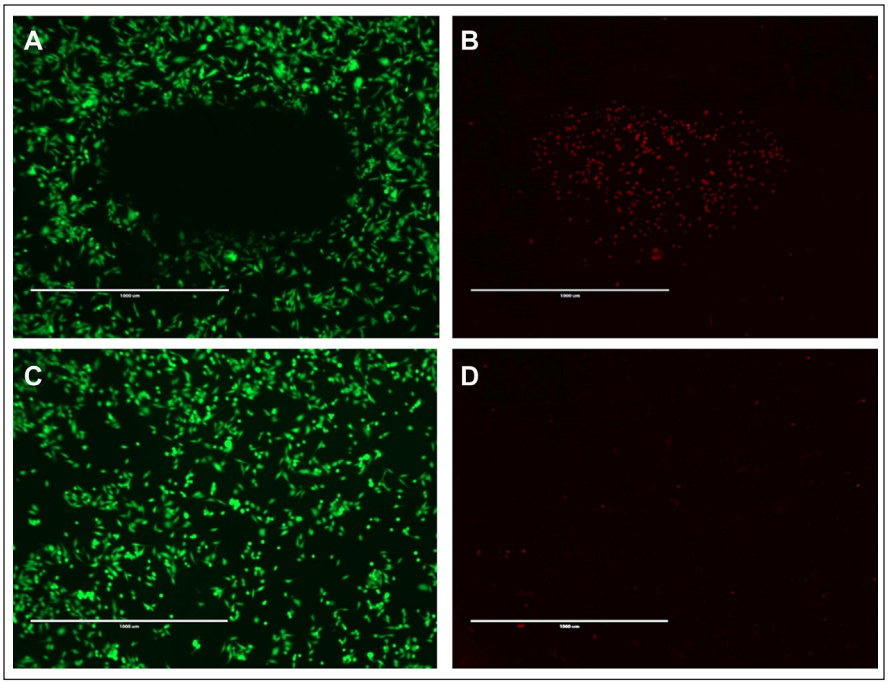

Figure 6. Cytotoxicity of (**A**, **B**) PC3 cells incubated with $K_{60}L_{20}$ gold nanoshells irradiated with a 200-mW, 808-nm laser diode and (**C**, **D**) PC3 cells only irradiated with the near-infrared laser. Live cells are stained green (**A**, **C**), and dead cells are stained red (**B**, **D**). Scale bar = 1 mm.

In conclusion, this article presents the first use of novel block copolypeptide vesicles as the core material for gold nanoshells. Using block copolypeptide vesicles as a core material has several advantages. Unlike traditional liposomes, polypeptide-based vesicles have a thicker membrane due to the longer polypeptide chains, which result in more stable vesicles. In addition, polypeptide-based vesicles have been shown to be biocompatible and stable under a variety of biological conditions. Furthermore, cargo can be loaded into the vesicles, which cannot be achieved using traditional silica-based gold nanoshells. However, one disadvantage to our synthesis method is the polydispersity of our vesicle population. Extrusion and the gold-coating protocol can be further optimized to address this problem. For example, parameters such as spin speed and ratio of gold to polypeptide can be further optimized. In this article, we have demonstrated the ability to coat the $K_{60}L_{20}$ vesicles with a thin layer of gold. The polypeptide-based gold nanoshells were found to generate significant heat in response to near-infrared light, which resulted in laser-induced, localized cancer cell death in vitro.

Acknowledgments

We also acknowledge the use of instruments in the Electron Imaging Center for Nanomachines core facility supported by the National Institutes of Health (1S10RR23057 and GM071940 to Z.H.Z.) and California NanoSystems Institute at UCLA.

Declaration of Conflicting Interests

The authors declared no potential conflicts of interest with respect to the research, authorship, and/or publication of this article.

Funding

The authors disclosed receipt of the following financial support for the research, authorship, and/or publication of this article: This work was supported by a grant from the National Science Foundation (DMR 1308081) to T.J.D. and D.T.K., as well as the National Science Foundation Graduate Research Fellowship (DGE-1144087) to K.M.M.

References

1. Huang, X.; El-Sayed, M. A. Gold Nanoparticles: Optical Properties and Implementations in Cancer Diagnosis and Photothermal Therapy. *J Adv. Res*. **2010**, *1*, 13–28.
2. Jain, P. K.; Lee, K. S.; El-Sayed, I. H.; et al. Calculated Absorption and Scattering Properties of Gold Nanoparticles of Different Size, Shape, and Composition: Applications in Biological Imaging and Biomedicine. *J. Phys. Chem B* **2006**, *110*, 7238–7248.
3. Link, S.; El-Sayed, M. A. Spectral Properties and Relaxation Dynamics of Surface Plasmon Electronic Oscillations in Gold and Silver Nanodots and Nanorods. *J. Phys. Chem. B* **1999**, *103*, 8410–8426.
4. Link, S.; El-Sayed, M. A. Shape and Size Dependence of Radiative, Non-Radiative and Photothermal Properties of Gold Nanocrystals. *Int. Rev. Phys. Chem*. **2000**, *19*, 409–453.
5. Qin, Z.; Bischof, J. C. Thermophysical and Biological Responses of Gold Nanoparticle Laser Heating. *Chem. Soc. Rev*. **2012**, *41*, 1191–1217.
6. Oldenburg, S.; Averitt, R.; Westcott, S.; et al. Nanoengineering of Optical Resonances. *Chem. Phys. Lett*. **1998**, *288*, 243–247.
7. Morton, J. G.; Day, E. S.; Halas, N. J.; et al. Nanoshells for Photothermal Cancer Therapy. *Methods Mol. Biol*. **2010**, *624*, 101–117.

8. Brown, K. R.; Natan, M. J. Hydroxylamine Seeding of Colloidal Au Nanoparticles in Solution and on Surfaces. *Langmuir* **1998**, *14*, 726–728.
9. Wu, C.; Yu, C.; Chu, M. A Gold Nanoshell with a Silica Inner Shell Synthesized Using Liposome Templates for Doxorubicin Loading and Near-Infrared Photothermal Therapy. *Int. J. Nanomed*. **2011**, *6*, 807–813.
10. Leung, S.; Romanowski, M. Light-Induced Release from Gold-Coated Liposomes. *Tech. Proc. 2011 NSTI Nanotechnol. Conf. Expo NSTI-Nanotech 2011* **2011**, *3*, 295–297.
11. Bardhan, R.; Grady, N. K.; Ali, T.; et al. Metallic Nanoshells with Semiconductor Cores: Optical Characteristics Modified by Core Medium Properties. *ACS Nano*. **2010**, *4*, 6169–6179.
12. FarrokhTakin, E.; Ciofani, G.; Puleo, G. L.; et al. Barium Titanate Core—Gold Shell Nanoparticles for Hyperthermia Treatments. *Int. J. Nanomed*. **2013**, *8*, 2319–2331.
13. Yong, K.-T.; Sahoo, Y.; Swihart, M. T.; et al. Synthesis and Plasmonic Properties of Silver and Gold Nanoshells on Polystyrene Cores of Different Size and of Gold–Silver Core–Shell Nanostructures. *Colloids Surfaces A Physicochem. Eng. Asp*. **2006**, *290*, 89–105.
14. Leung, S. J.; Kachur, X. M.; Bobnick, M. C.; et al. Wavelength-Selective Light-Induced Release from Plasmon Resonant Liposomes. *Adv. Funct. Mater*. **2011**, *21*, 1113–1121.
15. Troutman, T. S.; Leung, S. J.; Romanowski, M. Light-Induced Content Release from Plasmon Resonant Liposomes. *Adv. Mater*. **2009**, *21*, 2334–2338.
16. Wang, S.; Riahi, R.; Li, N.; et al. Single Cell Nanobiosensors for Dynamic Gene Expression Profiling in Native Tissue Microenvironments. *Adv. Mater*. **2015**, *27*, 6034–6038.
17. Riahi, R.; Wang, S.; Long, M.; et al. Mapping Photothermally Induced Gene Expression in Living Cells and Tissues by Nanorod-Locked Nucleic Acid Complexes. *ACS Nano*. **2014**, *8*, 3597–3605.
18. Holowka, E. P.; Pochan, D. J.; Deming, T. J. Charged Polypeptide Vesicles with Controllable Diameter. *J. Am. Chem. Soc*. **2005**, *127*, 12423–12428.
19. Sun, V. Z.; Choe, U.-J.; Rodriguez, A. R.; et al. Transfection of Mammalian Cells Using Block Copolypeptide Vesicles. *Macromol. Biosci*. **2013**, *13*, 539–550.
20. Holowka, E. P.; Sun, V. Z.; Kamei, D. T.; et al. Polyarginine Segments in Block Copolypeptides Drive Both Vesicular Assembly and Intracellular Delivery. *Nat. Mater*. **2007**, *6*, 52–57.
21. Lin, A. H.; Lewinski, N. A.; West, J. L.; et al. Optically Tunable Nanoparticle Contrast Agents for Early Cancer Detection: Model-Based Analysis of Gold Nanoshells. *J. Biomed. Opt*. **2005**, *10*, 064035.
22. Maeda, H.; Wu, J.; Sawa, T.; et al. Tumor Vascular Permeability and the EPR Effect in Macromolecular Therapeutics: A Review. *J. Control. Release*. **2000**, *65*, 271–284.
23. Krüger, A.; Kataoka, F.; Ozawa, M.; et al. Unusually Tight Aggregation in Detonation Nanodiamond: Identification and Disintegration. *Carbon* **2005**, *43*, 1722–1730.
24. Huang, X.; Jain, P. K.; El-Sayed, I. H.; et al. Determination of the Minimum Temperature Required for Selective Photothermal Destruction of Cancer Cells with the Use of Immunotargeted Gold Nanoparticles. *Photochem. Photobiol*. **2006**, *82*, 412–417.
25. Huang, H.-C.; Rege, K.; Heys, J. J. Spatiotemporal Temperature Distribution and Cancer Cell Death in Response to Extracellular Hyperthermia Induced by Gold Nanorods. *ACS Nano*. **2010**, *4*, 2892–2900.
26. Maksimova, I. L.; Akchurin, G. G.; Khlebtsov, B. N.; et al. Near-Infrared Laser Photothermal Therapy of Cancer by Using Gold Nanoparticles: Computer Simulations and Experiment. *Med. Laser Appl*. **2007**, *22*, 199–206.
27. Laszlo, A. The Effects of Hyperthermia on Mammalian Cell Structure and Function. *Cell Prolif*. **1992**, *25*, 59–87.
28. Lepock, J. R. Cellular Effects of Hyperthermia: Relevance to the Minimum Dose for Thermal Damage. *Int. J. Hyperthermia*. **2003**, *19*, 252–266.
29. Leung, S. J.; Kachur, X. M.; Bobnick, M. C.; et al. Wavelength-Selective Light-Induced Release from Plasmon Resonant Liposomes. *Adv. Funct. Mater*. **2011**, *21*, 1113–1121.